Vol 17 No 5, May 2008
1674-1056/2008/17(05)/1833-07

Chinese Physics B

© 2008 Chin. Phys. Soc.
and IOP Publishing Ltd

Light propagation characteristics in quantum well structures of photonic crystals*

Liu Jing(刘 靖)[a)b)], Sun Jun-Qiang(孙军强)[a)†], Huang Chong-Qing(黄重庆)[b)], Chen Min(陈 敏)[b)], and Huang De-Xiu(黄德修)[a)]

[a)] *Wuhan National Laboratory for Optoelectronics, School of Optoelectronics Science and Technology, Huazhong University of Science and Technology, Wuhan* 430074, *China*

[b)] *Hunan Institute of Science and Technology, Department of Physics, Yueyang* 414006, *China*

(Received 28 May 2007; revised manuscript received 18 September 2007)

Two-dimensional (2D) closed-cavity single quantum well (SQW) and multiple quantum well (MQW) structures are proposed based on the traditional 2D open-cavity SQW structures of photonic crystals. The numerical calculation results show that the proposed structures can greatly improve the optical characteristics compared with the traditional structures. It is found that the barrier thickness has a great impact on the optical characteristics of the closed-cavity MQW structures: when the barrier thickness is narrower, each resonant peak which appears in the SQW would split, the number of split times is just equal to the number of wells, and each well in the MQW structures is a travelling-wave-well, similar to the well in the open-cavity SQW structures; when the barrier thickness is wider, there is no effect of spectral splitting, and each well in the MQW structures is a standing-wave-well, just like the well in the closed-cavity SQW. The physical origin of different field distributions and the effect of the spectral splitting are provided.

Keywords: multiple quantum well, single quantum well, light field distribution, spectral splitting
PACC: 4270, 4870P, 3270

1. Introduction

Photonic crystals (PCs),[1,2] also known as photonic microstructures, have matured from an intellectual curiosity concerning electromagnetic waves into a field with real applications in the microwave and the optical regime since the end of the 1980s. The periodic modulation of the dielectric constant in these structures forms a photonic band gap (PBG) due to multiple Bragg scattering. Similar to semiconductor quantum well (QW) systems due to the electronic band gap mismatch, a photonic QW can be constructed by sandwiching an appropriate medium between two photonic barriers, the confined states which originate from the photonic confinement may be induced in PBG.[3,4] Their ability to control the flow of light and their capacity to concentrate light and enhance light-matter interaction are certainly inspiring. Many applications of photonic QW structures based on one-dimensional,[5,6] two-dimensional (2D)[7−9] and three-dimensional PCs[10−12] have been envisioned or realized.

Although a large number of papers have appeared on the photonic QW structures and the application of confined states in optical communication,[4−14] little consideration has been given to investigation of the spectral efficiency of PBG, and research on how to greatly improve the spectral transmissivities by only changing their own structures has not been seen until now. Especially, these published papers are mainly concentrated on SQW structures of PCs, but the papers on light field distribution in MQW structure of PCs are rarely seen. In fact, spectral efficiency is one of the primary concerns in the design of modern optical communication systems and the utilization of the associated communication channels due to the lack of spectral resources.[15] Simultaneously, the spectral intensity is an important parameter in designing highly effective optical devices.[16] And the photonic MQW structures may have many advantages compared with SQW structures, such as high-accuracy wavelength localization, strong ability of dispersion compensation, high luminous efficiency, and so on.[17]

In this paper, we construct the SQW and MQW structures with different light propagation characteristics by stacking the same construction units of two-

*Project supported by the National Natural Science Foundation of China (Grant Nos 60577006 and 50774034) and the Hunan Provincial Science Foundation of China (Grant No 06JJ20005).
†Corresponding author. E-mail: jqsun@mail.hust.edu.cn

dimensional PC. The FDTD method[18] is used to simulate transmission spectra and optical field distribution. Some measures which can greatly improve the light propagation characteristics are proposed. The performance of various photonic QW configurations is investigated and the device characteristics are related to the dynamics of capture, escape and localization of photons. The physical origin of different field distributions and the effect of the spectral splitting are provided.

2. Theoretical method

Our numerical simulation is based on finite-difference time-domain (FDTD) method with a perfectly matched layer absorbing boundary condition, which can be effectively used to calculate transmission spectra and field distributions of arbitrary-shape potential structures (for a detailed and exhaustive description, see Ref.[19]). By using this technique, photon propagation problems can be formulated systematically in terms of the well-known Maxwell's equations without using special mathematical knowledge. For simplicity, only the transverse-magnetic (TM) mode is investigated in the case of normal incidence. In what follows, only essential steps are outlined.

The basic research work is to compile accurate and effective FDTD computational procedures. The difference formulas used in programming are as follows:

$$E_z^{N+1}(i,j) = E_z^N(i,j) + \frac{\Delta t}{\varepsilon(i,j)\Delta x}\left[H_y^{N+1/2}\left(i+\frac{1}{2},j\right) - H_y^{N+1/2}\left(i-\frac{1}{2},j\right)\right] - \frac{\Delta t}{\varepsilon(i,j)\Delta y}\left[H_y^{N+1/2}\left(i,j+\frac{1}{2}\right) - H_y^{N+1/2}\left(i,j-\frac{1}{2}\right)\right], \quad (1)$$

$$H_y^{N+1/2}\left(i+\frac{1}{2},j\right) = H_y^{N-1/2}\left(i+\frac{1}{2},j\right) + \frac{\Delta t}{\mu(i,j)\Delta x}\left[E_z^N(i+1,j) - E_z^N(i,j)\right], \quad (2)$$

$$H_x^{N+1/2}\left(i,j+\frac{1}{2}\right) = H_y^{N-1/2}\left(i,j+\frac{1}{2}\right) - \frac{\Delta t}{\mu(i,j)\Delta x}\left[E_z^N(i,j+1) - E_z^N(i,j)\right], \quad (3)$$

where the subscripts i and j indicate the position of the grid point in the x- and the y- directions, respectively. N is the time step, $E_z^{N+1}(i,j)$ represents the electric field E_z at the corresponding position (i,j) and time step $N+1$, and the physical meanings of other field components can be analogized. $\varepsilon(i,j)$ and $\mu(i,j)$ are the position-dependent dielectric constant and the magnetic permeability of the material, respectively. Δt is the time increment, and $\Delta x = \Delta y = \Delta s$ is the spatial increment at neighbouring grid points along the x- and the y- directions. From the stability criterion, the duration of one time steps should satisfy the inequality $\Delta t \leq \Delta s/(c\sqrt{2})$. The time-varying electric fields at an observation point can be recorded in a digital group, and the transmission spectra can be obtained by taking the fast Fourier transform (FFT) of these recorded fields in a large range of frequencies. While the transmission spectra are calculated, modulation Gaussian pulse is chosen as an incident wave, and it is given by

$$E_z(t) = \cos(2\pi f_0 t) \times \exp\left[-4\pi\frac{(t-t_0)^2}{T^2}\right], \quad (4)$$

where f_0 is the central frequency of fundamental wave $\cos(2\pi f_0 t)$, t_0 is the central position of the Gaussian pulse, and T is the time constant. In this paper, we choose $t_0 = 20\Delta t$, and $T = 2\Delta t$. In order to favour the observation, in the calculated diagrammatic curves of transmission spectra, the frequencies described in x-coordinate are in reduced units, i.e. $\omega a/(2\pi \mathrm{c})$ is taken as their units with c being the light speed in vacuum, and ω the angular frequency. The y-coordinate values which represent the transmission coefficients can be calculated as the ratio of transmitted power to the incident power.

In the calculating of the optical field distributions, the simple harmonic wave is adopted, which can be expressed as the following expression:

$$E_z(t) = \cos(2\pi f_{\mathrm{m}} t), \tag{5}$$

where f_{m} is the frequency of the incident light. With the time step increasing, the electromagnetic field distributions in the well regions reach steady states gradually.

3. Light propagation characteristics in SQW structures

Figure 1(a) shows a schematic diagram which was frequently reported in Refs.[6,7] (called as "open-cavity SQW" in this paper). Both barriers, which are named "emission barrier" and "collection barrier", are formed with the same PC structures in the square lattices with a lattice constant a in the air. The cross section of the glass rods (black circle) is a circle with a radius $r = 0.25\,a$ and relative dielectric constant $\varepsilon_{\mathrm{r}} = 4.55$. These rods are placed along the z-direction, $\pm y$-directions are called side directions of SQW structures, and the thickness is finite in the x-direction. The potential well is formed by removing multiple-line rods from the centre of the two-dimensional PC; the left and the right sides of the potential well could act as potential barriers. The vacuum well thickness is $w = n \times a$, where n is the line number of the removed dielectric rods in the x-direction; the barrier thickness is $v = k \times a$, where k is the line number of rods in the barrier region in the x-direction. The light source is incident on the surface from the left in the case of normal incidence. Two detectors ($\mathrm{P_1}$ and $\mathrm{P_2}$) are placed on each side of the SQW, which can be used to measure the incident power and the transmission power, respectively. Thus, the transmissivity can be calculated readily as the ratio of the transmitted power to the incident power.

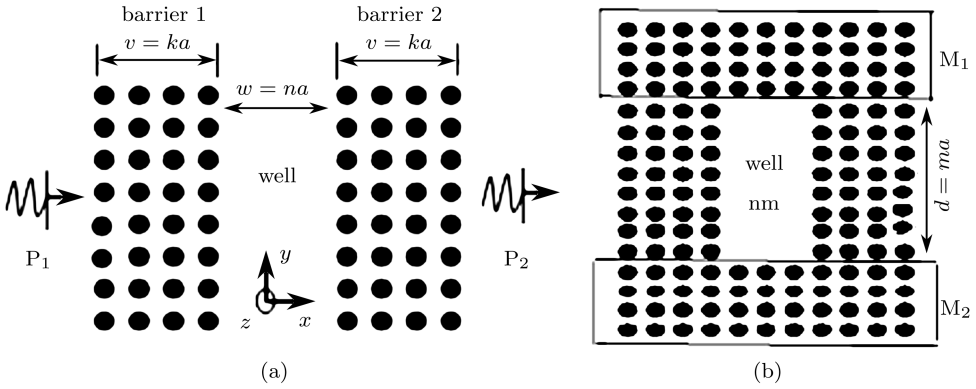


Fig.1. The schematics of the SQW structure: open-cavity SQW structure (a) and closed-cavity SQW structure (b).

We consider that in this open-cavity SQW, limited by the device volume, it is impossible for the size to be too large in the y-direction, thus the majority of the photons accumulated in the well region would radiate and leak out from the well as they are not restricted by any confinement effect, resulting in lower transmissivity. For this reason, we propose another photonic SQW structure by adding two periodic structures $\mathrm{M_1}$ and $\mathrm{M_2}$ in the side directions based on the open-cavity SQW as shown in Fig.1(b), which is called "closed-cavity SQW". The periodic structures $\mathrm{M_1}$ and $\mathrm{M_2}$ are also PC structures with the same geometric and dielectric parameters as those of the potential barriers. In this case, the size of the well region can be expressed as $m \times n$, where m is the number of rods removed from each line in the y-direction, thus the lateral length of the well is $d = m \times a$. We conjecture that once photons are trapped in the closed-cavity well, the probability for them to escape from the well would be very low due to the PBG around the well. In the present case, the total number of photons located in the well would increase. With the increase of energy, for some good reasons, the original condition with the low light field and the low transmissivity could be transformed into a new condition with a high light field and a high transmissivity.

In order to confirm our conjecture, we first calculate the transmission spectrum for the perfect 2D PC as shown in Fig.2(a). It is clearly observed that the first PBG is from 0.33 to 0.45. Next, we calculate the transmission spectra of open-cavity SQW and closed-cavity SQW structures with $v = 4\,a$ and $w = 3\,a$ as shown in Figs.2(b) and 2(c), respectively. It is clearly seen that resonant peaks will emerge inside PBG in which it is impossible for guided modes to appear. These calculated peaks cannot be explained as the

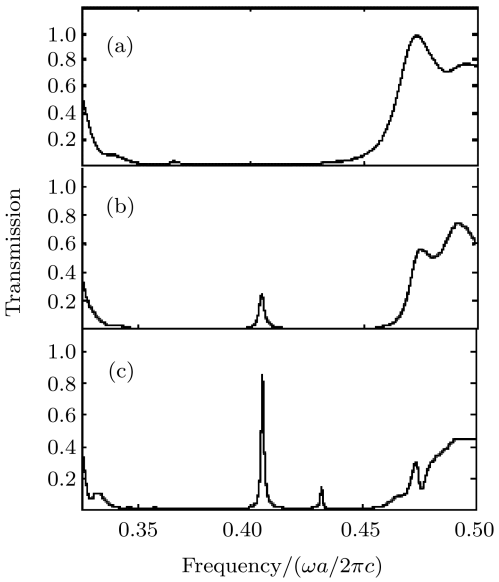


Fig.2. Transmission spectra for the perfect 2D PC (a), the open-cavity SQW structure (b), and the closed-cavity SQW structure (c).

quantized states of the photonic band but as impurity states of PC due to the effects of the quantum size and the resonant tunnelling. We see that with the same well thickness and barrier thickness, the numbers of sharp peaks for both SQW structures are the same, and their corresponding positions remain nearly unchanged. But the transmissivity of the open-cavity SQW structure is obviously weaker; the output light intensity is lower; the frequency selectivity is poorer; the quality factor Q is smaller. These results firmly confirm our conjecture, i.e. the closed-cavity QW could bound photons more strongly as mentioned above.

To further explore the physical origin of the difference in spectral intensity, the optical field distributions of these open-cavity and closed-cavity SQW structures at a normalized resonance frequency of 0.406 are calculated as shown in Figs.3(a) and 3(b). In these figures, the x- and the y-axes take a lattice constant a as the size of their unit cell, and the z-axis represents the optical field intensity and takes V/m as the size of its unit cell. Figure 3(a) indicates that the well in the open-cavity SQW is a travelling-wave-well, in which the distribution of light intensity exhibits a Gaussian distribution, and the gradient of potential field is smaller. Thus, the capability for the well to capture photons is weak. In this case, the majority of the photons accumulated in the well will radiate or leak out and go into the free air. This is the main reason for the open-cavity QW to have a low transmissivity. Figure 3(b) indicates that the well in a closed-cavity QW structure is a standing-wave-well, in which a Gaussian wave envelopes with a big light field gradient can be obtained in the wavelength dimension, leading to the strong confinement for photons. That is to say, the paths for photons to escape from the well are blocked up, and photons are frozen at some discrete energy levels. Thus, each energy level could obtain more photons and a high transmissivity. For this reason, in the following text, only closed-cavity MQW structures are considered.

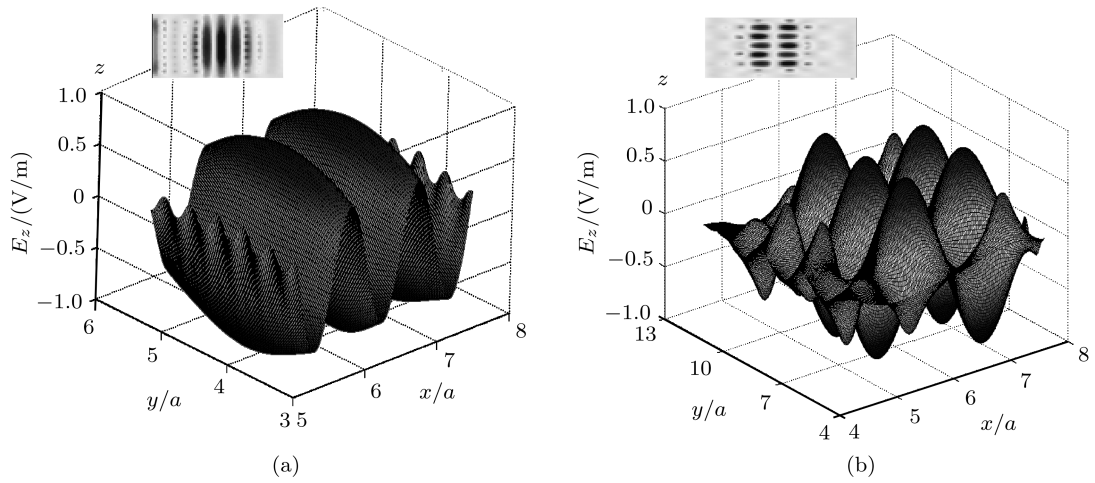


Fig.3. The field distributions for open-cavity SQW (a) and closed-cavity SQW (b) with insets for the false-colour image of the optical field distribution.

Note that each inset in Fig.3(a) shows a false-colour image of the corresponding optical field distribution. By transforming three-dimensional graphics into two-dimensional graphics, we can obtain the field distribution from the step grey scale simply but clearly. So it is shown in Fig.3(b) and the next field distribution graphics.

4. Light propagation characteristics in MQW structures

First, we consider the case in which the barrier thickness between adjacent wells is narrow. Figures 4(a) and 4(b) are the schematics of closed-cavity double QW (DQW) structure and closed-cavity triple QW (TQW) structure with a narrower-barrier thickness, respectively. Each of them can be regarded as the cascade connection of multiple SQW structures.

Figures 5(a) and 5(b) show the transmission spectra of DQW structure and TQW structure with $v = 4\,a$ and $w = 3\,a$, respectively. By analysing the different transmission peaks shown in Figs.2(c), 5(a) and 5(b) carefully, we can see that in the SQW structure, only one spectrum is produced; with a narrower thickness, in the DQW structure, two spectral lines are produced; in TQW structures, three spectral lines are produced; ····· the more the number of QW, the more the spectral lines are produced. We call this effect 'spectral splitting'. That is to say, each resonant peak which appears in the SQW would split: the number of split times is just equal to that of wells, those split peaks are un-folded. In this way, the number of the confined states can be multiplied in the limited PBG region, leading to a high spectral efficiency in PBG. If the number of wells is large enough, each split region can turn into a sub-energy band, which is important for optical devices in communications.

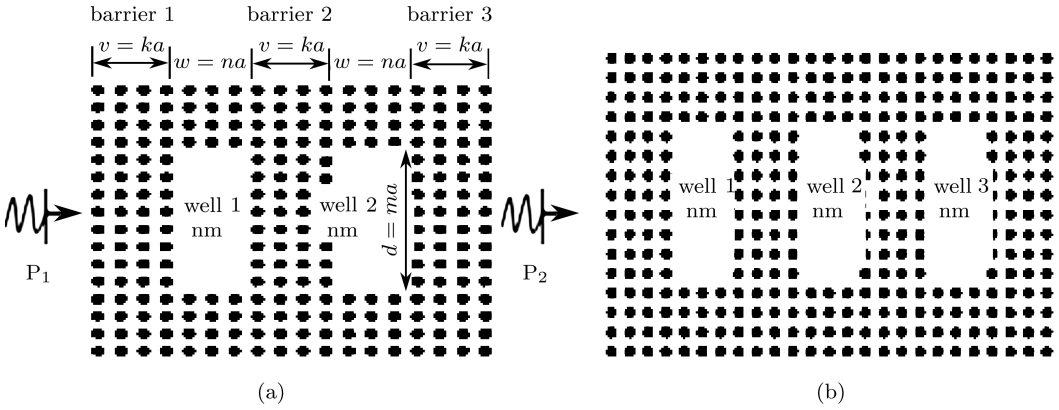


Fig.4. The schematics of MQW structures with a narrower thickness for closed-cavity DQW (a) and closed-cavity TQW (b).

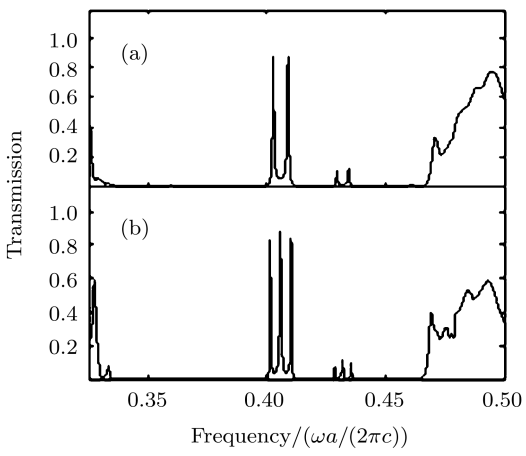


Fig.5. Transmission spectra with a narrower barrier thickness for closed-cavity DQW (a) and closed-cavity TQW (b).

Figures 6(a) and 6(b) are the field distributions of DQW and TQW at normalized resonance frequencies of 0.409 and 0.411, respectively. Each well in the DQW and TQW structures is a travelling-wave-well. This can be explained as follows: while the barrier thickness is smaller than the penetration depth of wave function, the wave function penetrates into the barrier regions, leading to the mutual overlap of wave functions between adjacent wells. In this case, photon states located in different wells may be related to each other coherently through the tunnelling effect; this made the case in which the photons located at single-level could go through different wells. Simultaneously, the quantum states in different potential wells may interact and couple mutually, resulting in

the splitting of the degenerate energy level located in the SQW structure. The frequency interval between the split spectra is determined by the strength of interactions between wells.

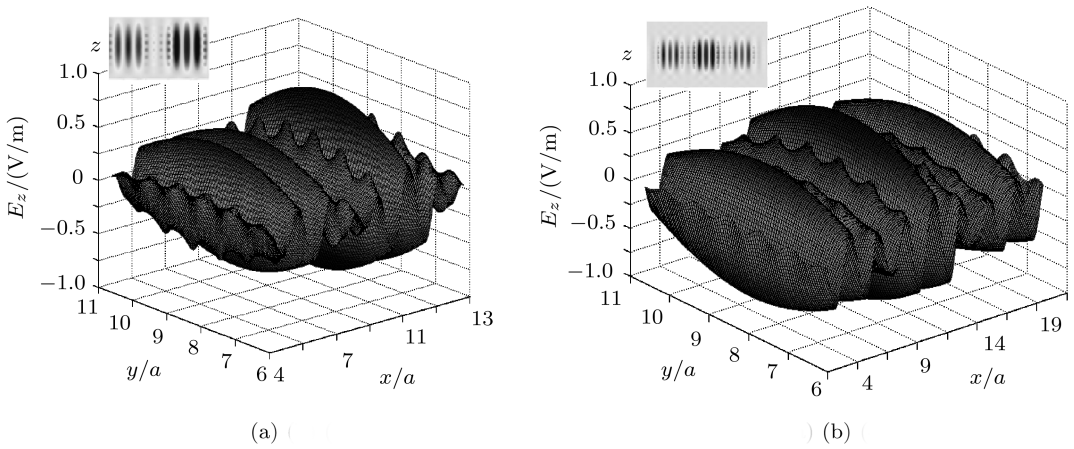


Fig.6. The field distributions with a narrower barrier thickness for closed-cavity DQW (a) and closed-cavity TQW (b) with insets for the false-colour image of the optical field distribution.

Next, we consider the case in which the barrier thickness between adjacent wells is wide. According to the MQW structures with a narrower barrier thickness, we can easily construct the MQW structures with a wider barrier thickness by only doubling the barrier thickness, while other geometric and dielectric parameters are exactly the same as those chosen in Fig.4. In this case, the calculated transmission spectra show that there is no effect of spectral splitting. This characteristic is completely different from that shown in Fig.5. Owing to the limited length of this paper, the corresponding structures and transmission spectra are not presented here.

Figures 7(a) and 7(b) are the field distributions of these wider barrier DQW and TQW structures each at a normalized resonance frequency of 0.406. It indicates that in the case of wider barrier thickness between adjacent wells, each well in the closed-cavity DQW and TQW structures is a standing-wave-well, and each Gaussian envelope located in one well cannot migrate to the other wells. The physical origin of these results may be explained as follows: while the barrier thickness is far wider than the penetration depth of wave functions, wave functions are mainly bounded in the wells, and the mutual overlap of wave functions between adjacent wells may be ignored. Thus, many

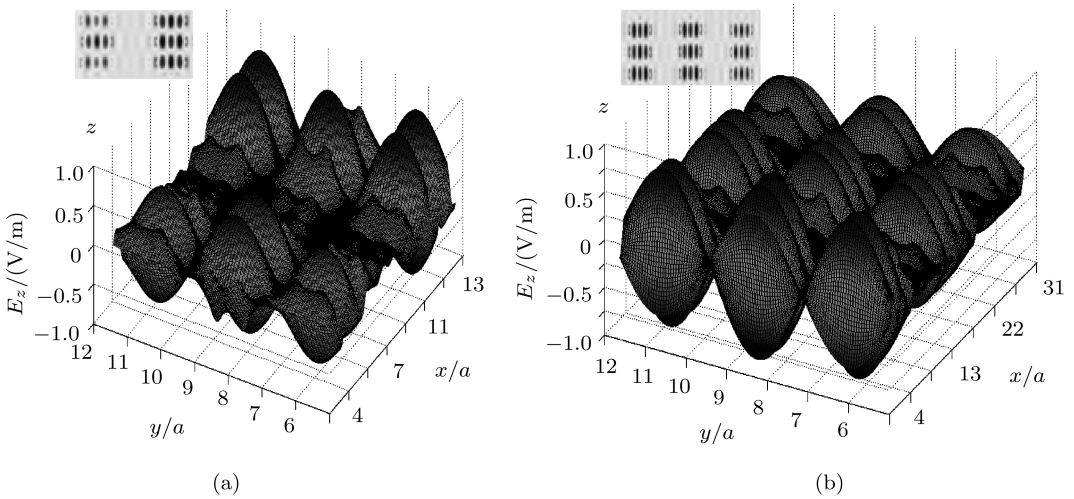


Fig.7. The field distributions with a wider barrier thickness for closed-cavity DQW (a) and closed-cavity TQW (b) with insets for the false-colour image of the optical field distribution.

physical properties of MQW structures may be characterized through the corresponding properties of isolated wells.

Finally, we should mention that a less number of wells are involved in the earlier discussion. The general conclusions, however, can be applied to four QW, five QW, and so on.

5. Conclusion

We have studied theoretically the propagation and the confinement of optical wave in SQW and MQW structures. Our results show that the closed-cavity QW structure can improve the transmission efficiency of photons compared with open-cavity QW structure. It is found that the barrier thicknesses between adjacent wells have a tremendous influence on the optical characteristics of the closed-cavity MQW structures; while the barrier thickness is narrow, each well in the MQW structures is a travelling-wave-well, similar to the well in the open-cavity SQW structures, each resonant peak which appears in the SQW would split, and the number of split times is just equal to the number of wells; while the barrier thickness is wider, each well in the MQW structures is a standing-wave-well without the effect of spectral splitting, just like the well in the closed-cavity SQW. The conclusions drawn from this work could provide theoretical guideline to designing and producing optical communication devices, such as the laser source, the super narrow-band filter, the optical coupler, and so on.

References

[1] Yablonovitch E 1987 *Phys. Rev. Lett.* **58** 2059

[2] John S 1987 *Phys. Rev. Lett.* **58** 2486

[3] Joannopoulos J D, Meade R D and Winn J N 1995 *Photonic Crystals: Molding the Flow of Light* (Princeton, NJ: Princeton University Press) pp38–76

[4] Hong C X, Sheng L X, Quan S and Shun Z N 2007 *Acta Phys. Sin.* **56** 2742 (in Chinese)

[5] Yoon J, Lee W, Caruge J M, Bawendi M, Thomas E L, Kooi S and Prasad P N 2006 *Appl. Phys. Lett.* **88** 091102

[6] Liu J, Sun J Q, Huang D X, Huang C Q and Wu M 2007 *Acta Phys. Sin.* **56** 2281 (in Chinese)

[7] Jiang Y, Niu C and Liu D L 1999 *Phys. Rev.* B **59** 9981

[8] Tian J, Ren C, Feng S, Liu Y Z, Tao H H, Li Z Y, Cheng B Y, Zhang D Z and Jin A Z 2006 *Chin. Phys.* **15** 2471

[9] Pan Y, Li Z F and Chen X S 2006 *J. Infrared Millim. Waves* **25** 17

[10] Yano S, Segawa Y and Bae J S 2001 *Phys. Rev.* B **63** 153316

[11] Wang J, Yuan C W and Tang F Q 2005 *Chin. Phys.* **14** 1581

[12] Diop M, Maurin G, Tork A and Lessard R A 2002 *Opt. Eng.* **41** 1943

[13] Li S G, Xing G L, Zhou G Y, Han Y, Hou L T, Hu M L, Li Y F and Wang Q Y 2006 *Chin. Phys.* **15** 437

[14] Qiao F, Zhang C and Wan J 2000 *Apll. Phys. Lett.* **77** 3698

[15] Sagias N C, Varzakas P, Tombras G S and Karagiannidis G K 2005 *Journal of the Franklin Institute* **342** 7

[16] Song J O, Leem D S, Kwak J S, Park Y, Chae S W and Seong T Y 2005 *Photon. Technol. Lett.* **17** 291

[17] Ramey S M and Khoie R 2003 *IEEE Trans. Electron Devices* **50** 1179

[18] Yee K S 1966 *IEEE Trans. Antennas Propagat.* **14** 302

[19] Taflove A and Hagness S C 2000 *Computational Electrodynamics: The Finite-Difference Time-Domain Method* (Boston, MA: Artech House)